JOURNAL OF ENVIRONMENTAL SCIENCES 99 (2021) 267–273

Available online at www.sciencedirect.com

ScienceDirect

www.elsevier.com/locate/jes

JES JOURNAL OF ENVIRONMENTAL SCIENCES

www.jesc.ac.cn

Enhanced degradation of organic contaminants using catalytic activity of carbonaceous structures: A strategy for the reuse of exhausted sorbents

Kalyani Mer[1], *Baharak Sajjadi*[2,*], *Nosa.O. Egiebor*[1], *Wei-Yin Chen*[2], *Daniell.L. Mattern*[3], *Wendong Tao*[1]

[1] *Environmental Resources Engineering Department, SUNY College of Environmental Science and Forestry, Syracuse, NY 13210, USA*

[2] *Department of Chemical Engineering, School of Engineering, University of Mississippi, MS 38677-1848, USA*

[3] *Department of Chemistry and Biochemistry, University of Mississippi, MS 38677, USA*

ARTICLE INFO

Article history:
Received 16 April 2020
Revised 11 June 2020
Accepted 24 June 2020
Available online 17 July 2020

Keywords:
Biochar
Graphitic carbons
Persistent free radicals (pfrs)
Advanced oxidation process (aop)
Hydrogen peroxide
Phenol

ABSTRACT

Generation of hydroxyl radicals (·OH) is the basis of advanced oxidation process (AOP). This study investigates the catalytic activity of microporous carbonaceous structure for in-situ generation of ·OH radicals. Biochar (BC) was selected as a representative of carbon materials with a graphitic structure. The work aims at assessing the impact of BC structure on the activation of H_2O_2, the reinforcement of the persistent free radicals (PFRs) in BC using heavy metal complexes, and the subsequent AOP. Accordingly, three different biochars (raw, chemically- and physiochemically-activated BCs) were used for adsorption of two metal ions (nickel and lead) and the degradation of phenol (100 mg/L) through AOP. The results demonstrated four outcomes: (1) The structure of carbon material, the identity and the quantity of the metal complexes in the structure play the key roles in the AOP process. (2) the quantity of PFRs on BC significantly increased (by 200%) with structural activation and metal loading. (3) Though the Pb-loaded BC contained a larger quantity of PFRs, Ni-loaded BC exhibited a higher catalytic activity. (4) The degradation efficiency values for phenol by modified biochar in the presence of H_2O_2 was 80.3%, while the removal efficiency was found to be 17% and 22% in the two control tests, with H_2O_2 (no BC) and with BC (no H_2O_2), respectively. Overall, the work proposes a new approach for dual applications of carbonaceous structures; adsorption of metal ions and treatment of organic contaminants through *in-situ* chemical oxidation (ISCO).

Introduction

Hydrogen peroxide (H_2O_2) has been effectively used for the remediation of diverse kinds of organic contaminants via *in-situ* chemical oxidation processes (Xue et al., 2012). Although H_2O_2 is a very strong oxidant, its direct reaction with organic contaminants is generally slow. Hence, it is often subjected to certain activation agents including heat, UV radiation, metal-based activation, etc. (Devi et al., 2016; Zhang et al., 2020; Zhu et al., 2020). The activation of H_2O_2 leads to the formation of hydroxyl (•OH) radicals, which further react with the target contaminants resulting in their degradation (Devi et al., 2016). Recently, activated carbon combined with H_2O_2 has been used in the generation of •OH radicals to degrade organic contaminants present in water and wastewater systems (Karthikeyan et al., 2015). H_2O_2 interacts with the activated carbon surface to generate free •OH

* Corresponding author.
E-mail: bsajjadi@olemiss.edu (B. Sajjadi).

https://doi.org/10.1016/j.jes.2020.06.030
1001-0742/

radicals through an electron transfer mechanism, similar to Fenton's reaction (Rey et al., 2016). The ability of activated carbons to induce the formation of free ·OH radicals from H_2O_2 has been attributed to the graphitic structures and the iron content of the activated carbons.

Biochar, the carbonaceous residue derived from thermal decomposition of biomass, exhibits properties similar to activated carbon and contains some resonance-stabilized radicals known as persistent free radicals (PFRs), such as, semiquinones, cyclopentadienyls, and phenoxyls (Fang et al., 2015). PFRs are formed by the thermal decomposition of organic compounds like hydroquinones, catechols, and phenols in the presence of metal oxides (e.g., CuO, Fe_2O_3) through an electron-transfer mechanism (Dellinger et al., 2007; Fang et al., 2014b). The type and concentration of PFRs vary with the operating pyrolysis temperature used for the production of biochar (Fang et al., 2014a). PFRs are resonance stabilized and can promote the catalytic decomposition of H_2O_2 to ·OH radicals (Qin et al., 2018; Khachatryan et al., 2011). Semiquinone-type PFRs can transfer an electron to molecular oxygen resulting in the formation of superoxide radical ion, which further induces Fenton reactions to produce ·OH radicals in the presence of silica/CuO particles (Khachatryan and Dellinger, 2011).

The PFRs generation on biochar surface can be enhanced by loading BC with metal or metal oxide nano particles (NP) (Fu et al., 2017; Yu et al., 2015). For example, it was found that Cr(VI) remediation facilitated the formation of PFRs on rice husk derived biochar (Zhang et al., 2019). Fu et al. reported a 97.8% removal efficiency for tetracycline using a solid-digestate-biochar-Cu NP-based composite activator system for H_2O_2 (Fu et al., 2017). It has been reported that electron transfer between biochar and metal ions increases the formation of PFRs on biochar surface (Kiruri et al., 2014; Yan et al., 2020). However, their formation in the presence of metal ions generally requires a heating treatment prior to pollutant removal (Zhang et al., 2019). While formation of PFRs without thermal treatment has not been studied, it likely has a profound effect in their behaviour and fate.

A previous study performed by our group has shown that the physical treatment of biochar with ultrasound radiation followed by chemical functionalization can significantly improve its adsorption capacity towards heavy metals, mainly Ni^{2+} (Sajjadi et al., 2019a). Ultrasonic treatment exfoliates the biochar's graphitic clusters, facilitates the leaching of mineral compounds and creates new micropores, thus increasing the surface area and porosity significantly and improving the functionalization efficiency and the adsorption capacity. Therefore, this study aims to (1) use physically and chemically treated biochar for removal of two heavy metal ions (Ni and Pb) from water as a model for wastewater remediation; (2) explore the ability of the adsorbed metal to increase the quantity of PFRs on biochar; and (3) investigate the catalytic activity of the metal-loaded biochar for *in-situ* activation of H_2O_2 and ensuing degradation of an organic contaminant. Phenol was selected as a model contaminant since it is a priority pollutant in the EPA list because of its high toxicity and resistance to biodegradation.

1. Materials and methods

Biochar-Now Company (Berthoud Colorado, USA) supplied raw biochar for the experiments. The feedstock used for this biochar is softwood pine; its pyrolysis was accomplished at temperatures ranging between 823 K and 873 K in an oxygen-deprived environment in a kiln reactor. The activating acid was phosphoric acid (H_3PO_4, 85%) and the functionalizing agent was diethanolamine DEA ($C_4H_{11}NO_2$, > 98%, solid). The heavy metals to be adsorbed, nickel ($NiCl_2$, 98%, powder) and lead ($PbCl_2$, 98%, powder); the phenol (C_6H_6O, >99%) for AOP studies; and hydrogen peroxide (H_2O_2, 30%) were purchased from Sigma-Aldrich. For adsorption experiments, the various test kits, including nickel (TNTplus 856), lead (TNTplus 850), and phenol (TNTplus 868), were ordered from Hach. All water used for dilutions was deionized water purchased from Walmart.

Biochar activation, characterization, metal adsorption and advanced oxidation (AOP) experiments were explained in the supplementary information. In short, three different categories of activated biochars were synthesized: (1) Ultrasono-modified biochar without any kind of chemical treatment or functionalization (US-BC); (2) Chemically activated biochar without any acoustic treatment (BC-P and BC-P-DEA), and (3) Chemically activated biochar with ultrasonic treatment (US-BC-P-DEA and US-BC-P-DEA). In metal adsorption experiments, solutions including 100 mg/L Ni(II) or Pb(II) were treated with 0.5 g of activated biochar for 8 hr. AOP tests were then conducted using mixtures including 0.1 g of metal-loaded biochar and phenol solution (100 mg/L) in presence of 1 mL of 30% H_2O_2.

Table 1 – Surface area analysis of raw and acoustic-activated biochars before metal adsorption and (sono)-chemically activated biochars after metal adsorption.

Biochar ID	BET surface area (m^2/g)	Porosity (cc/g)	t-plot micropore area (m^2/g)
Raw	196.10	0.101	149.68
US-BC	175.60	0.086	168.07
BC + Ni	155.55	0.073	143.82
BC + Pb	128.04	0.069	119.30
US-BC + Ni	146.12	0.071	114.11
US-BC + Pb	101.85	0.058	86.00
US-BC-P-DEA + Ni	58.44	0.031	55.74
US-BC-P-DEA + Pb	13.57	0.007	8.16

2. Results and discussions

2.1. Surface area analysis

The surface area and porosity of biochar affect its adsorption capacity, and thus the mechanisms involved in the metal removal process (Li et al., 2017; Yu et al., 2015); for example, biochar with relatively small pore size is inefficient in trapping a large adsorbate, regardless of the surface charges or polarity (Khare et al., 2017). Biochar surface area generally tends to increase with pyrolysis temperature (Abbas et al., 2018). However, it can also be modified through physical activations such as acoustic treatment (Table 1). The results indicate that micropore surface area of raw biochar increased as a result of sonication, suggesting the creation of new micropores into the biochar structure. Meanwhile, BET surface area and meso-porosity of raw biochar showed a reduction due to the conversion of meso pores into micro-pores. Increase of micropore surface area and reduction of macro-pore area upon sonication have been observed in our previous works as well (Sajjadi et al., 2019a). Increased micropore area favours chemical functionalization, as it provides suitable channels for the chemical compounds to converge on the lower layers of the carbonaceous structure. The meso and micro surface areas and porosity of both raw and activated biochar reduced significantly after the adsorption of nickel or lead metal ions. This reduction was more prominent in Pb^{2+} loaded samples due to higher adsorption of lead ions into biochar structure. The ultrasono-chemically activated/functionalized biochar with adsorbed lead metal ions had the lowest surface area and pore volume, clearly indicating the positive effect of chemical activation and functionalization on the adsorption of metal ions onto the biochar surface (as suggested by elemental analysis as well), though this reduction could also be partly attributed to the coating of DEA on BC.

2.2. SEM Analysis

The changes in the surface morphologies of raw (Fig. 1a) and sonicated biochar (Fig. 1b) were exhibited by SEM imaging. As observed, the surface textures of the raw biochar contained irregular patterns of blocked pores, which could result from residues of the formation of volatile compounds and ash during the pyrolysis of the cellular

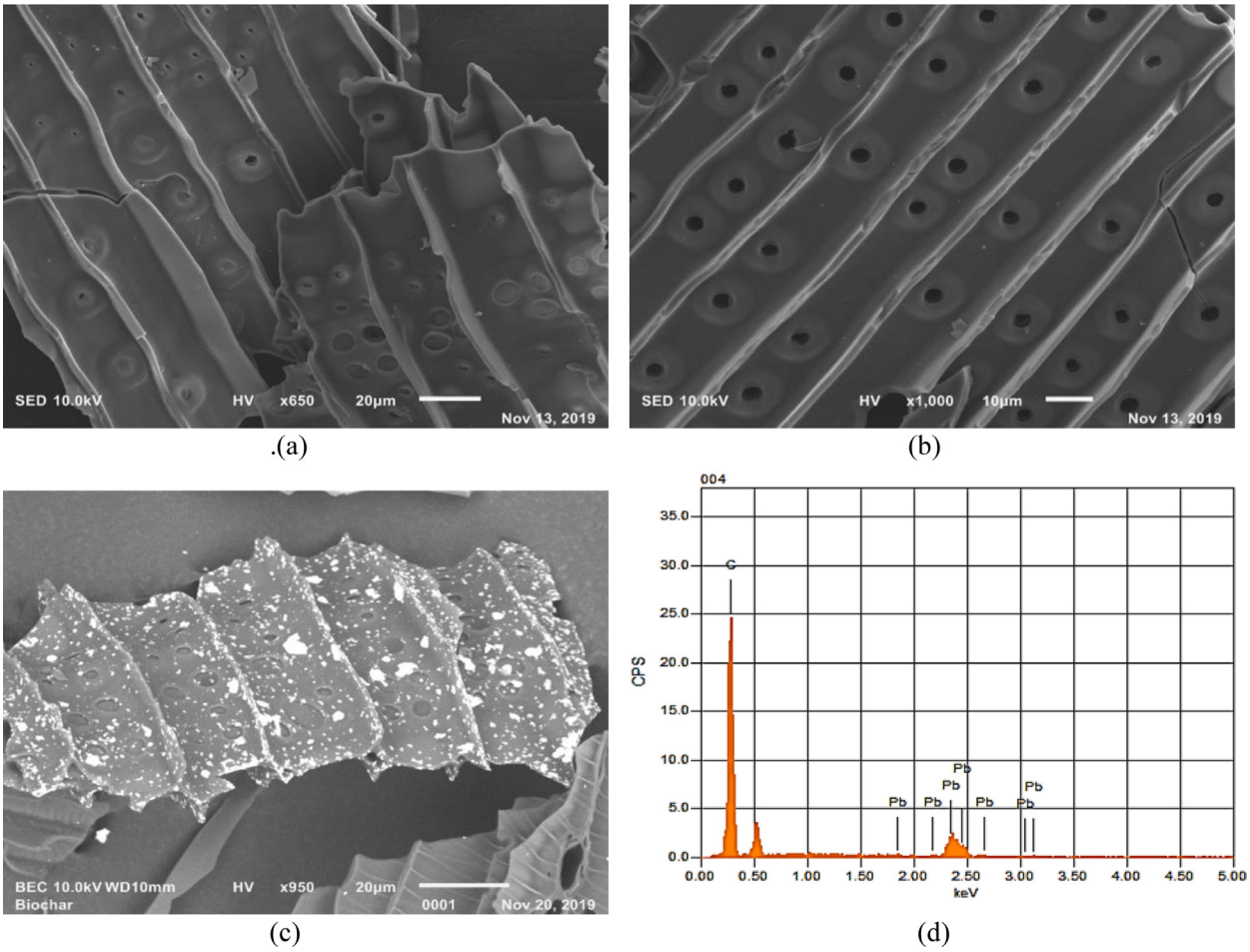

Fig. 1 – Scanning electron micrograph showing the surface morphology of (a) raw biochar and (b) ultrasound treated biochar, (c) lead-loaded biochar taken in backscattered electron mode (BED-C), (d) showing the presence of different elements based on atomic number contrast. Bar = 20 µm, working distance (WD) = 11 mm, accelerating voltage (AV) = 10.0 kV, spot size (SS) = 50, SED.

structure of the biomass (Fig. 1a). On being treated with ultrasound, there was a generation of new micropores, or the opening of blocked ones, resulting in an increase in the biochar's porosity and surface area (Fig. 1b). In addition to the development of new pores, ultrasonic exposure imparts a cleaning effect on the biochar surface by removing various lumps present on the unmodified biochar, even in underlayers, thus resulting in a smoother and more even surface. SEM images of lead-loaded biochar (Fig. 1c) and a point analysis (Fig. 1d) revealed the heavy metal ions trapped onto the surface of biochar. This observation is in accordance with the surface area analysis results of metal-loaded biochar showing a significant decrease in biochar surface areas after metal adsorption.

2.3. *Elemental Analysis*

The content of elements composing raw, modified and metal-loaded BCs are listed in Table 2. Low contents of lead and nickel were observed in samples that were not treated with metal. The quantity of lead was significantly lower in the ultrasound activated sample (US-BC) compared to raw BC, which could reflect the reduction of ash content (from 4.13% to 3.22%). Low contents of P were observed in samples that were not treated with phosphoric acid (raw BC: 389 µg/g; BC treated with Ni: 365 µg/g or Pb: 305 µg/g). The P contents were further reduced in their corresponding ultra-sonicated biochars (US-BC: 292 µg/g, US-BC treated with Ni: 323 µg/g) except for the P content of raw BC treated with Pb, which was almost equal to its corresponding ultra-sonicated BC: 308 µg/g. It should be noted that ash contains Na, Mg, K, Ca, P and other mineral elements (Sajjadi et al., 2019b). Due to a significant reduction of ash, the highest reduction of P content is observed in US-BC compared to raw BC, both untreated with any metal. Upon metal treatment, the quantity of absorbed metal increased in both BC and US-BC samples. The quantity of Pb assayed in metal-treated US-BC was almost 5-times that of Ni (around 10,000 versus 2,000 µg/g). Due to the difference atomic masses of the metals, this represents a 1.4-fold higher amount of lead on an atomic basis. Whether the BC was raw and ultrasonicated made little difference in the mass of metal observed, in spite of higher micro-porosity of the US-BC. This is attributed to the leaching of adsorbed metal during long durations of adsorption (8 hr). In other words, US-BC initially adsorbed higher quantities of metal, mainly through physical adsorption; however, eventual leaching of adsorbed metals is inevitable due to the lack of sufficient functional groups on these biochars.

Similar behaviour was observed in acid-treated biochar. However, treatment with phosphoric acid lowered the metal loading of both pristine (BC-P) and acoustic-activated BC (US-BC-P) to approximately 40% of those in BC and US-BC. As expected, phosphorous content of the samples increased after acidic treatment. By further functionalization using DEA, the average nitrogen content of BCs significantly increased from 0.36% to 1.21%, indicating the successful attachment of DEA, which subsequently increased Pb and Ni adsorption/loading on the functionalized BCs. Accordingly, the maximum of Ni and Pb was observed in US-BC-P-DEA, which include 34% and 66% more Ni and Pb, respectively, compared to BC-P-DEA. This observation sug-

Table 2 – Elemental compositions (dry basis) of raw and activated biochar samples with/without metal adsorption.

Sample ID	Metal adsorption	Carbon % w/w	Hydrogen % w/w	Nitrogen % w/w	Oxygen % w/w	Ash % w/w	Lead (μg/g)	Nickel (μg/g)	Phosphorus (μg/g)
BC	–	79.99	2.66	0.28	14.37	4.13	30	5	389
US-BC	–	80.93	2.72	0.28	13.08	3.22	13	4	292
BC	Ni^{2+}	80.00	2.73	0.29	12.98	3.42	22	1940	365
BC	Pb^{2+}	79.95	2.80	0.50	13.73	3.49	10500	8	305
US-BC	Ni^{2+}	80.05	2.75	0.50	13.28	3.40	16	2040	323
US-BC	Pb^{2+}	79.76	2.79	0.53	13.04	3.83	10100	8	308
BC-P	Ni^{2+}	81.41	2.83	0.30	12.95	1.99	7	657	744
BC-P	Pb^{2+}	81.25	2.88	0.33	13.28	2.18	3640	8	801
US-BC-P	Ni^{2+}	81.26	2.95	0.31	14.02	1.51	33	701	1130
US-BC-P	Pb^{2+}	80.55	2.89	0.33	14.10	2.72	3020	10	1050
BC-P-DEA	Ni^{2+}	78.60	3.27	1.20	15.77	2.03	6	4570	766
BC-P-DEA	Pb^{2+}	79.53	3.12	1.16	14.47	2.27	8600	10	723
US-BC-P-DEA	Ni^{2+}	79.79	3.09	1.21	15.52	1.97	8	6140	564
US-BC-P-DEA	Pb^{2+}	78.45	3.12	1.27	15.05	2.79	14300	11	542

gests the prominent advantage of acoustic activation prior to acid-treatment and DEA-functionalization.

2.4. *FT-IR analysis*

FT-IR spectra of raw and modified biochar with and without metal loading are shown in Fig. 2. CO_2 stretching provides a common peak observed in all the spectra at 2350 cm^{-1}. The strong and broad peak between 3200 and 3550 indicates the stretching of surface hydroxyl (-OH) groups. The two bands between 2850 and 2950 indicate the symmetrical or asymmetrical stretching vibration of $–CH_3$ and $–CH_2$ groups of aliphatic hydrocarbons, and it can be noted that both these peaks are enhanced in the samples containing heavy metals. The small peak at around 2690 could represent C-H (aldehyde) stretching. The bands at 1600-1730 indicate the stretching vibrations of carboxyl or carbonyl C=O groups or C=C bonds in aromatic rings.

It was observed that active functional groups, such as phenolic hydroxyl (C-OH) and carboxylic (COOH) are involved in metal ions adsorption. Upon adsorption of Pb(II) and Ni(II), a new peak appeared at 1384 cm^{-1}. This was due to the symmetric stretches of COO- complexed with metal ions (Ibrahim et al., 2005; Papageorgiou et al., 2010). Similarly, the bands at 1110 and 1180 cm^{-1} are related to C-O stretching vibrations; they are less prominent in the spectra of raw and ultrasound-treated biochars without any metal. The strong absorption at 2125 is likely an overtone of this signal (Mozgawa et al., 2009). The peaks at 1180 (the asymmetric stretch of C-O-H) and 1110 cm^{-1} (the symmetric stretch of C-O-H) (Shi et al., 2018) also increased, respectively, after the complexation of metal ions in the current study.

Fig. 3 presents the adsorption efficiencies of raw and activated biochars towards lead and nickel, within 1 and 8 hr. Metal removal, the mechanisms of metal ion adsorption and the impact of physical activation using low-frequency ultrasound irradiation, acidic pretreatment and functionalization have been discussed in detail in our previous studies (Sajjadi et al., 2019a; Sajjadi et al., 2020). Accordingly, just the results of the test conducted for this study are provided here and more discussion can be found in Appendix A.

2.5. *PFR Analysis*

The Electron Paramagnetic Resonance (EPR) spectra in Fig. 4 demonstrate the persistent free radical content of raw and acoustic-activated biochars before and after metal adsorptions. The presence of PFRs in raw bicohar (red line) was reduced as a result of ultrasound activation and hence the minimum intensity of PFRs was observed in US-BC. Biochar has graphite and graphitic oxide clusters that consist of the different functional groups, such as hydroxyl (-OH), aldehyde -((C=O)H) and carboxyl -((C=O) OH). Metal oxides are the other important source of PFRs in biochar, which are generated

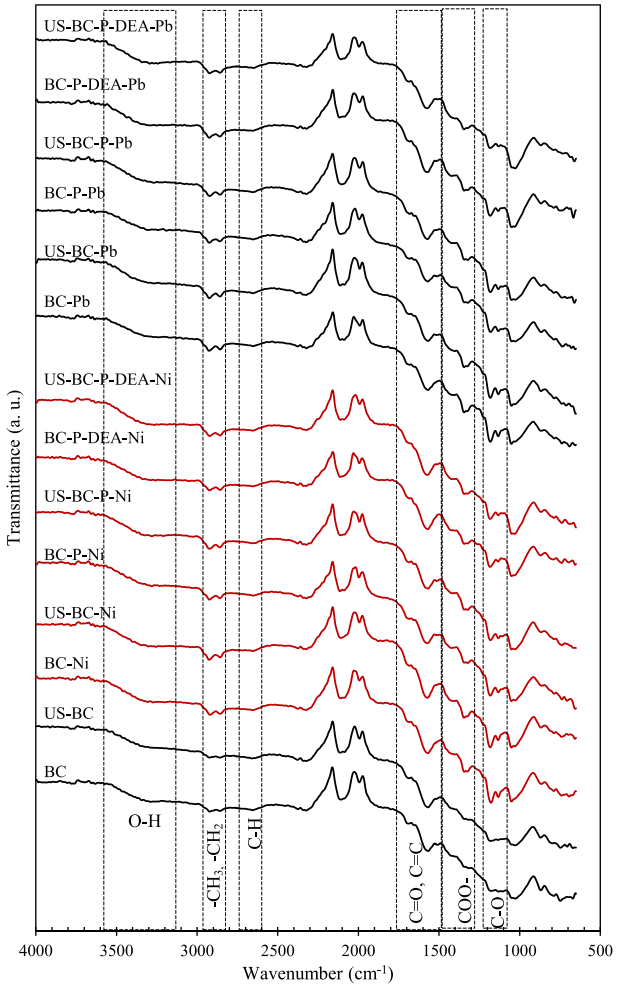

Fig. 2 – FT-IR analysis showing the effect of ultrasound activation, phosphoric acid treatment, DEA functionalization and metal adsorption on the formation of PFR in Ni^{2+} and Pb^{2+}-loaded biochar.

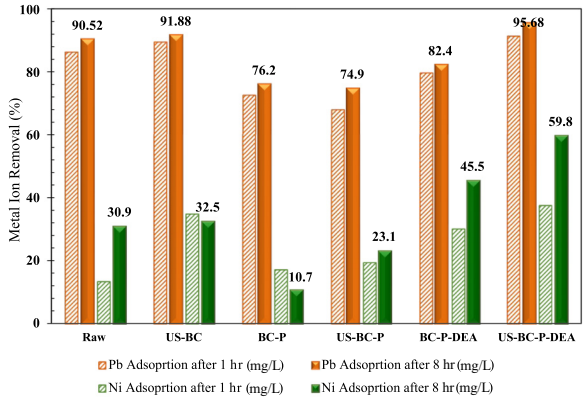

Fig. 3 – The effect of ultrasound activation, phosphoric acid treatment and DEA functionalization on adsorption of Ni^{2+} and Pb^{2+} by biochar within 1 and 8 hr.

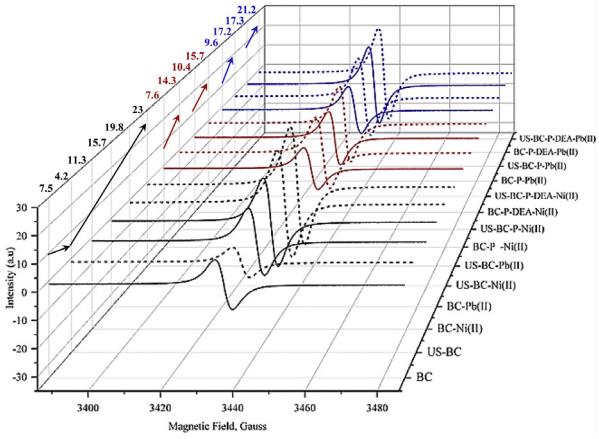

Fig. 4 – EPR spectra showing the effect of ultrasound activation, phosphoric acid treatment, DEA functionalization and metal adsorption on the formation of PFR in Ni^{2+} and Pb^{2+}-loaded biochar.

during pyrolysis of biomass. Hence the PFRs on biochar were likely a mixture of carbon and oxygen-centered radicals (Zhang et al., 2019). Fang et al (Fang et al., 2015) reported that the PFR concentration rapidly increased with pyrolysis time at 300 and 400°C, while it markedly reduced to below detection limit for pyrolysis at 500 and 600°C. The nature of this reduction can be attributed to the decomposition and removal of reactive oxygen containing functional groups. A similar phenomenon occurs under ultrasound irradiation. Acoustic activation tends to remove a significant number of functional groups, particularly oxygen-containing groups (as also confirmed with oxygen content of BC, Table 2), which subsequently reduces the oxygen-centered PFRs of biochar. The mechanisms of possible radical reactions on the edge site of biochar with hydroxyl and hydrogen radicals in ultrasound irradiated aqueous solution was studied in our previous work (Zubatiuk et al., 2017). According to reaction pathways, the energy diagrams, and the computed enthalpy change, ΔH of the reaction of hydrogen and hydroxyl radicals with an edged carbon is exothermic and barrierless. However, the loss of $HO^{\bullet}$ is about 12 kcal/mol more favorable than H desorption from the same carbon site. Both simulation (Zubatiuk et al., 2017) and experimental results suggest that oxygen content is reduced upon ultrasound activation while hydrogen content increases. In addition, ultrasound activation facilitates the leaching of mineral compounds (ash) from biochar structure, which are mainly in the oxidized form.

As also shown in Fig. 4, the PFR concentration increased sharply with metal loading, particularly in Pb loaded BCs. These results suggest that metal loading (or adsorption of heavy metals) would participate in the formation of PFRs in biochar. Most of the previous studies on the formation of PFRs (Khachatryan et al., 2011) suggest the key role of thermal treatment of organic compounds in the presence of metal oxides followed by electron transfer from the adsorbate to the metal atom. Although PFR formation without heating treatment has not been investigated yet, this could be one of the important missing features in PFR behaviour; the results of the current study show the possibility of PFR formation upon metal chemisorption on carbonaceous adsorbent even without thermal treatment. In addition, in contrast with the PFR content observed in raw and acoustic-activated samples, the latter showed a more intense PFR peak for all samples after metal adsorption. This effect, though, could not be attributed solely to the loading of metals after acoustic activation, since the elemental analysis (Table 2) and adsorption results (Fig. 3) do not show any significant difference between the Pb or Ni content of the raw and acoustic-activated BC. Accordingly, the higher PFR content of US-BC following metal treatment must be partly due to the structure changes of biochar after physical activation under ultrasound.

Generally, the concentrations of PFRs in Pb-loaded samples were higher than those containing Ni. This is attributed to the greater content of Pb in biochar structure, as also was suggested by elemental contents of biochar (Table 2) and the Pb adsorption. The lowest content of PFRs was observed in the phosphoric acid treated biochars BC-P-Ni and BC-P-Pb, which contained the lowest quantity of nickel and lead. The concentrations of PFRs increased markedly for the DEA-functionalized samples. Again, this impact was significantly enhanced by acoustic activation. These results suggest that acoustic activation synergistically boosted the effect of metal loading on PFR, even though ultrasound treatment alone reduced the PFR content of biochar. Accordingly, the maximum content of PFRs was observed for US-BC-P-DEA-Pb and US-BC-Pb; which were 177 and 197% above the PFR signal of raw biochar, respectively.

2.6. *Possible mechanisms of PFR formation and H_2O_2 decomposition by BC*

According to previous studies (Fang et al., 2014a; Devi et al., 2016), the chemisorption and oxidation of organic pollutants and the reduction of quinones, or the oxidation of phenolic hydroxyls, to form phenoxyl radicals are the two possible sources of generation of PFRs Because no organic pollutants were used in this study, the increase of PFRs can be attributed redox reactions between Pb^{2+} or Ni^{2+} and reactive functional groups on biochar. Fig. 5 proposes the conversion of a metal adsorbed on biochar to a PFR. PFR formation proceeds through a 3-step mechanism including: physisorption, chemisorption with the elimination of H_2O, and electron transfer to form a reduced metal along with the PFRs on the carbonaceous surface. The resulting PFRs may be both oxygen-centered and carbon-centered, as represented by the two resonance forms in Fig. 5, with the major form depending on the properties of the PFR-metal complex.

Biochar and H_2O_2 have a three-way interaction with each other. Firstly, H_2O_2 oxidizes biochar (Nie et al., 2019); secondly, H_2O_2 decomposes over carbon surfaces and forms free radicals; and thirdly, PFRs of biochar can reduce O_2 to H_2O_2 (Yang et al., 2017).

Biochar or activated carbon catalyze the conversion of H_2O_2 to $HO^{\bullet}$ by one-electron reduction (Fang et al., 2014a; Yang et al., 2017) that resembles the Fenton reactions:

$$C_m^{\bullet} + H_2O_2 \rightarrow C_m(+) + HO^{\bullet} + OH^- \quad (1)$$

$$C_m(+) + H_2O_2 \rightarrow C_m^{\bullet} + HO_2^{\bullet} + H^+ \quad (2)$$

Positive correlation has been reported between the concentrations of $HO^{\bullet}$ and the initial concentration of PFRs. On the other hand, significant reduction of PFR concentration has also been observed after reaction with H_2O_2. In addition, the decomposition rate of H_2O_2 is proportional to the quantity of hydroxyl groups on the biochar surface. These observations suggest that PFRs might participate in the production of $HO^{\bullet}$ from H_2O_2 with biochar (Fang et al., 2014a, 2014b).

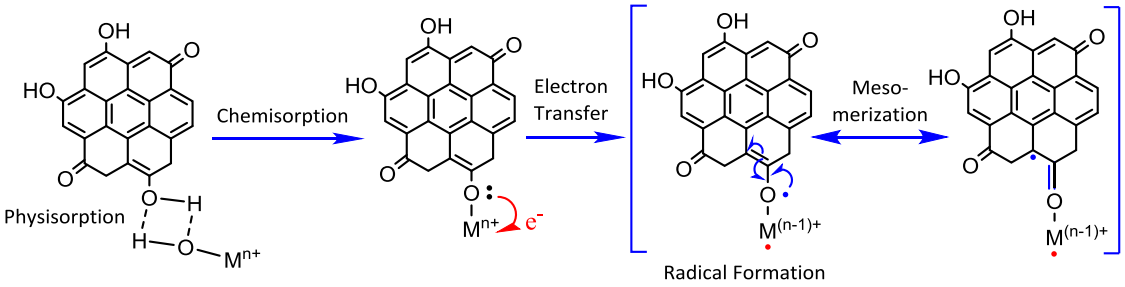

Fig. 5 – Proposed Mechanism of PFR formation from a metal adsorbed on biochar, developed based on the previous publications (Fang et al., 2014a; Balakrishna et al., 2009; Lomnicki et al., 2008). M^{n+}: Transition metal.

Not only do the PFRs of BC play a key role in H_2O_2 decomposition and HO• generation, but BC PFRs may also convert ambient oxygen into H_2O_2, for example by β-elimination of adsorbed O_2 (Reaction (3)) (Yang et al., 2017). This provides an additional source of H_2O_2 which can then back-react with the BC to generate HO•. In addition, oxygen covalently bonded to a PFR could eliminate another reactive oxygen species, peroxyl radical $HO_2^{\bullet}$ (Reaction (4)). Electron transfer from hydroquinone or semiquinone groups to oxygen could produce $O_2^{-\bullet}$ (Reaction (5)), as could electron transfer from carbon-centered radicals (Reaction (6)). The combination of two radical species, as in (Reaction (7)), would remove them as reactants, but would generate another H_2O_2 to continue the AOP (Yang et al., 2017).

$$C_m(O_2) + H_2O \rightarrow C_m(-2H^+) + H_2O_2 \quad (3)$$

$$C_m(OO^{\bullet}) + H_2O \rightarrow C_m(-H^+) + HO_2^{\bullet} \quad (4)$$

$$\text{hydroquinone, semiquinone} + O_2 \rightarrow \text{semiquinone, quinone} + O_2^{-\bullet} \quad (5)$$

$$C_m^{\bullet} + O_2 + H_2O \rightarrow C_m(-H^+) + O_2^{-\bullet} \quad (6)$$

$$HO_2^{\bullet} + O_2^{-\bullet} + H_2O \rightarrow H_2O_2 + O_2 + OH^- \quad (7)$$

2.7. AOP study

To investigate the possibility of H_2O_2 activation by metal-loaded biochar, the oxidative degradation of phenol was studied under different conditions. Fig. 6 shows that after 4 hr of reaction time, phenol removal efficiency was 21.7% for raw biochar (BC) and 28.1% for ultrasound treated biochar (US-BC), with the removal essentially complete after 15 min. This slight increase in phenol removal efficiency on addition of US-BC can be attributed to better adsorption of phenol on the surface of biochar. The raw BC and US-BC (without any adsorbed metal), when used in combination with H_2O_2, resulted in a decreased concentration of phenol. However, after 15 min of reaction time an increase in the concentration was observed for the BC-H_2O_2 sample (Appendix A Figure 9bS), reaching a peak value at about 1 hr. It was followed by a decrease in concentration until 2 hr of reaction time, after which the concentration of phenol remained almost constant. Overall, the removal efficiency of phenol was 32.9% for BC-H_2O_2 and 37.9% for US-BC-H_2O_2 systems. In the activator (metal-biochar) - H_2O_2 systems, the phenol removal efficiency reached up to 40.9% and 32.8% on addition of nickel- and lead-loaded BCs, respectively. A further increase in the removal efficiency was observed on using metal-loaded US-BC combined with H_2O_2, with a value of 43.2% for nickel and 38.6% for lead loading. This can be possibly attributed to increased adsorption of both the heavy metals, which further enhanced the formation of PFRs on the biochar surface, hence improving the phenol removal process. A slight reduction was then observed in phenol degradation by acid-treated samples (except for BC-P-Pb). It could also be attributed to the reduced adsorption of metal ions. Ultimately, the highest removal efficiencies of phenol were found for H_2O_2 biochar combinations involving ultrasound treated, phosphoric acid activated, amine functionalized, metal loaded biochar. As displayed in Appendix A Figures

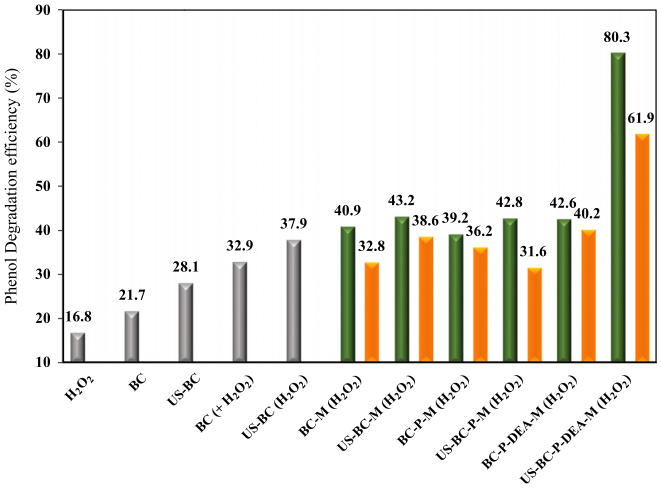

Fig. 6 – Phenol degradation in control tests: H_2O_2 (without BC), BC and US-BC (without H_2O_2) and using different activated BCs in presence of H_2O_2. M: Transition metal loaded. ■ Ni(II), ■ Pb(II).

9 and 9bS, approximately 80.3% of phenol was removed in 4 hr when nickel-loaded, fully activated biochar was used in combination with H_2O_2. In case of the lead-loaded biochar activator system, the phenol removal efficiency approached a value of 62%. These results reflect that nickel-loaded modified biochar (US-BC-P-DEA-Ni^{2+}) exhibited the most effective activation of H_2O_2.

Two points must be highlighted. (1) As already discussed, Pb-loaded samples (US-BC-P-DEA-Pb^{2+} and US-BC-Pb^{2+}) contained the maximum quantity of PFRs. In contrast, the highest degradation of phenol was observed by nickel-loaded biochars, suggesting that the activity (or identity) of the PFRs plays a key role in this process rather than only their quantity. However, the impact of US activation on BC structure cannot be eliminated. (2) Georgi and Kopinke (2005) revealed that the reaction of the organic contaminants with HO• has the superior influence for degradation in the AC (Activated Carbon)/H_2O_2 system in the aqueous phase. Since the adsorbed contaminant is nearly unreactive with the HO•, the adsorption is detrimental to degradation by HO•. In contrast, Yang et al. (2016, 2017) showed that addition of a radical scavenger to remove HO• did not completely suppress the decomposition of p-nitrophenol (PNP), indicating that surface reaction of PNP with both radical and non-radical sites is likely an important contributor to PNP degradation. The results of the current study demonstrated 20%-30% of phenol adsorption with raw BS and US-BS, even in the absence of H_2O_2 or, in other words, HO•.

3. Conclusion

The results of this study suggested that biochar exhibited enhanced reactivity in decomposing H_2O_2 to generate $^{\bullet}OH$ through the activity of persistent free radicals; the concentration of PFRs increased after the adsorption of heavy metals onto the biochar surface; and metal-loaded BC (biochar) could efficiently be used for an *in-situ* oxidation process (ISOP). The increased formation of PFRs in metal-loaded biochar was confirmed through EPR studies and their contribution in enhancing the oxidative activity of BC was suggested by the degradation of phenol in aqueous solution through ISOP in the metal-loaded BC-H_2O_2 system. However, although Pb-loaded BCs contained the highest quantity of PFRs, the maximum phenol degradation was observed in Ni-loaded BCs. Therefore, the type or activity of PFRs generated was the other key. Metal loading appeared to participate in the formation of PFRs in biochar, even without thermal treatment. However, the impact of a secondary thermal treatment on PFR formation needs further studies. Overall, this study provides a novel approach to manipulate the PFR content of carbonaceous structures and suggest a new strategy to reuse biochar after heavy metal adsorption in the catalytic decomposition/oxidation of organic contaminants.

Acknowledgements

The authors are grateful for the financial support of the National Science Foundation (NSF EPSCoR RII Grant No. OIA-1632899). Also, the authors would like to acknowledge Ohio Advanced EPR laboratory at Miami University for helping in accomplishing the PFR analyses and N.C. Brown Center for Ultrastructure studies, SUNY-ESF for SEM analysis.

Appendix A Supplementary data

Supplementary material associated with this article can be found, in the online version, at doi:10.1016/j.jes.2020.06.030.

REFERENCES

Balakrishna, S., Lomnicki, S., McAvey, K.M., Cole, R.B., Dellinger, B., Cormier, S.A., 2009. Environmentally persistent free radicals amplify ultrafine particle mediated cellular oxidative stress and cytotoxicity. Part. Fibre. Toxicol. 6, 11. doi:10.1186/1743-8977-6-11.

Dellinger, B., Lomnicki, S., Khachatryan, L., Maskos, Z., Hall, R.W., Adounkpe, J., et al., 2007. Formation and stabilization of persistent free radicals. Proc. Combust. Inst. 31, 521–528. doi:10.1016/j.proci.2006.07.172.

Devi, P., Das, U., Dalai, A.K., 2016. *In-situ* chemical oxidation: Principle and applications of peroxide and persulfate treatments in wastewater systems. Sci. Total Environ. 571, 643–657. doi:10.1016/j.scitotenv.2016.07.032.

Fang, G.D., Gao, J., Liu, C., Dionysiou, D.D., Wang, Y., Zhou, D., 2014a. Key Role of Persistent Free Radicals in Hydrogen Peroxide Activation by Biochar: Implications to Organic Contaminant Degradation. Environ. Sci. Technol. 48, 1902–1910. doi:10.1021/es4048126.

Fang, G.D., Liu, C., Gao, J., Dionysiou, D.D., Zhou, D., 2015. Manipulation of Persistent Free Radicals in Biochar To Activate Persulfate for Contaminant Degradation. Environ. Sci. Technol. 49, 5645–5653. doi:10.1021/es5061512.

Fang, G.D., Liu, C., Gao, J., Zhou, D., 2014b. New Insights into the Mechanism of the Catalytic Decomposition of Hydrogen Peroxide by Activated Carbon: Implications for Degradation of Diethyl Phthalate. Ind. Eng. Chem. Res. 53, 19925–19933. doi:10.1021/ie504184r.

Fu, D., Chen, Z., Xia, D., Shen, L., Wang, Y., Li, Q., 2017. A novel solid digestate-derived biochar-Cu NP composite activating H_2O_2 system for simultaneous adsorption and degradation of tetracycline. Environ. Pollut. 221, 301–310. doi:10.1016/j.envpol.2016.11.078.

Georgi, A., Kopinke, F.D., 2005. Interaction of adsorption and catalytic reactions in water decontamination processes: Part I. Oxidation of organic contaminants with hydrogen peroxide catalyzed by activated carbon. Appl. Catal. B 58, 9–18. doi:10.1016/j.apcatb.2004.11.014.

Ibrahim, M., Nada, A., Kamal, D.E., 2005. Density functional theory and FTIR spectroscopic study of carboxyl group. IJPAP 43 (12) December 2005.

Karthikeyan, S., Boopathy, R., Sekaran, G., 2015. *In situ* generation of hydroxyl radical by cobalt oxide supported porous carbon enhance removal of refractory organics in tannery dyeing wastewater. J. Colloid Interface Sci. 448, 163–174. doi:10.1016/j.jcis.2015.01.066.

Khachatryan, L., Dellinger, B., 2011. Environmentally Persistent Free Radicals (EPFRs)-2. Are Free Hydroxyl Radicals Generated in Aqueous Solutions? Environ. Sci. Technol. 45, 9232–9239. doi:10.1021/es201702q.

Khachatryan, L., Vejerano, E., Lomnicki, S., Dellinger, B., 2011. Environmentally Persistent Free Radicals (EPFRs). 1. Generation of Reactive Oxygen Species in Aqueous Solutions. Environ. Sci. Technol. 45, 8559–8566. doi:10.1021/es201309c.

Khare, P., Dilshad, U., Rout, P.K., Yadav, V., Jain, S., 2017. Plant refuses driven biochar: Application as metal adsorbent from acidic solutions. Arab. J. Chem. 10, S3054–S3063. doi:10.1016/j.arabjc.2013.11.047.

Kiruri, L.W., Khachatryan, L., Dellinger, B., Lomnicki, S., 2014. Effect of Copper Oxide Concentration on the Formation and Persistency of Environmentally Persistent Free Radicals (EPFRs) in Particulates. Environ. Sci. Technol. 48, 2212–2217. doi:10.1021/es404013g.

Li, H., Dong, X., Silva, E.B., de Oliveira, L.M., Chen, Y., Ma, L.Q., 2017. Mechanisms of metal sorption by biochars: Biochar characteristics and modifications. Chemosphere 178, 466–478. doi:10.1016/j.chemosphere.2017.03.072.

Lomnicki, S., Truong, H., Vejerano, E., Dellinger, B., 2008. Copper Oxide-Based Model of Persistent Free Radical Formation on Combustion-Derived Particulate Matter. Environ. Sci. Technol. 42, 4982–4988. doi:10.1021/es071708h.

Nie, T., Hao, P., Zhao, Z., Zhou, W., Zhu, L., 2019. Effect of oxidation-induced aging on the adsorption and co-adsorption of tetracycline and Cu^{2+} onto biochar. Sci. Total Environ. 673, 522–532. doi:10.1016/j.scitotenv.2019.04.089.

Papageorgiou, S.K., Kouvelos, E.P., Favvas, E.P., Sapalidis, A.A., Romanos, G.E., Katsaros, F.K., 2010. Metal–carboxylate interactions in metal–alginate complexes studied with FTIR spectroscopy. Carbohyd. Res. 345, 469–473. doi:10.1016/j.carres.2009.12.010.

Qin, Y., Li, G., Gao, Y., Zhang, L., Ok, Y.S., An, T., 2018. Persistent free radicals in carbon-based materials on transformation of refractory organic contaminants (ROCs) in water: A critical review. Water Res. 137, 130–143. doi:10.1016/j.watres.2018.03.012.

Rey, A., Hungria, A.B., Duran-Valle, C.J., Faraldos, M., Bahamonde, A., Casas, J.A., et al., 2016. On the optimization of activated carbon-supported iron catalysts in catalytic wet peroxide oxidation process. Appl. Catal. B 181, 249–259. doi:10.1016/j.apcatb.2015.07.051.

Sajjadi, B., Broome, J.W., Chen, W.Y., Mattern, D.L., Egiebor, N.O., Hammer, N., et al., 2019a. Urea functionalization of ultrasound-treated biochar: A feasible strategy for enhancing heavy metal adsorption capacity. Ultrason. Sonochem. 51, 20–30. doi:10.1016/j.ultsonch.2018.09.015.

Sajjadi, B., Chen, W.Y., Egiebor, N.O., 2019b. A comprehensive review on physical activation of biochar for energy and environmental applications. Rev. Chem. Eng. 35, 735–776. doi:10.1515/revce-2017-0113.

Sajjadi, B., Chen, W.Y., Mattern, D.L., Hammer, N., Dorris, A., 2020. Low-temperature acoustic-based activation of biochar for enhanced removal of heavy metals. J. Water Process Engin. 34, 101166. doi:10.1016/j.jwpe.2020.101166.

Shi, Q., Sterbinsky, G.E., Prigiobbe, V., Meng, X., 2018. Mechanistic Study of Lead Adsorption on Activated Carbon. Langmuir 34, 13565–13573. doi:10.1021/acs.langmuir.8b03096.

Xue, Y., Gao, B., Yao, Y., Inyang, M., Zhang, M., Zimmerman, A.R., et al., 2012. Hydrogen peroxide modification enhances the ability of biochar (hydrochar) produced from hydrothermal carbonization of peanut hull to remove aqueous heavy metals: Batch and column tests. Chem. Engin. J. 200–202, 673–680. doi:10.1016/j.cej.2012.06.116.

Yan, J., Yang, L., Qian, L., Han, L., Chen, M., 2020. Nano-magnetite supported by biochar pyrolyzed at different temperatures as hydrogen peroxide activator: Synthesis mechanism and the effects on ethylbenzene removal. Environ. Pollut. 261, 114020. doi:10.1016/j.envpol.2020.114020.

Yang, J., Pan, B., Lsi, H., Liao, S., Zhang, D., Wu, M., et al., 2016. Degradation of p-Nitrophenol on Biochars: Role of Persistent Free Radicals. Environ. Sci. Technol. 50, 694–700. doi:10.1021/acs.est.5b04042.

Yang, J., Pignatello, J.J., Pan, B., Xing, B., 2017. Degradation of p-Nitrophenol by Lignin and Cellulose Chars: H2O2-Mediated Reaction and Direct Reaction with the Char. Environ. Sci. Technol. 51, 8972–8980. doi:10.1021/acs.est.7b01087.

Yu, Z., Zhou, L., Huang, Y., Song, Z., Qiu, W., 2015. Effects of a manganese oxide-modified biochar composite on adsorption of arsenic in red soil. J. Environ. Manag. 163, 155–162. doi:10.1016/j.jenvman.2015.08.020.

Zhang, X.Y, Sun, P., Wei, K., Huang, X., Zhang, X.Y., 2020. Enhanced H_2O_2 activation and sulfamethoxazole degradation by Fe-impregnated biochar. Chem. Engin. J. 385, 123921. doi:10.1016/j.cej.2019.123921.

Zhang, K., Sun, P., Zhang, Y., 2019. Decontamination of Cr(VI) facilitated formation of persistent free radicals on rice husk derived biochar. Front. Environ. Sci. Eng. 13, 22. doi:10.1007/s11783-019-1106-7.

Zhu, L., Ji, J., Liu, J., Mine, S., Matsuoka, M., Zhang, J., et al., 2020. Designing 3D-MoS2 Sponge as Excellent Cocatalysts in Advanced Oxidation Processes for Pollutant Control. Angewandte Chemie International Edition, doi:10.1002/anie.202006059.

Zubatiuk, T., Sajjadi, B., Hill, G., Leszczynska, D., Chen, W.Y., Leszczynski, J., 2017. Modeling radical edge-site reactions of biochar in CO_2/water solution under ultrasonic treatment. Chem. Phys. Lett. 689, 48–55. doi:10.1016/j.cplett.2017.09.058.